SCIENTIFIC REPORTS

OPEN

SUBJECT AREAS:
REACTION MECHANISMS
COMPUTATIONAL CHEMISTRY
STRUCTURE PREDICTION
ELECTRONIC STRUCTURE

Received
12 November 2012

Accepted
29 January 2013

Published
14 February 2013

Correspondence and requests for materials should be addressed to X.Z. (xzhao@mail.xjtu.edu.cn) or X.G. (gaox@ihep.ac.cn)

Two-Dimensional Carbon Compounds Derived from Graphyne with Chemical Properties Superior to Those of Graphene

Jia-Jia Zheng[1,2], Xiang Zhao[1], Yuliang Zhao[2] & Xingfa Gao[2,3]

[1]Institute for Chemical Physics & Department of Chemistry, State Key Laboratory of Electrical Insulation and Power Equipment, Xi'an Jiaotong University, Xi'an 710049, China, [2]CAS Key Laboratory for Biomedical Effects of Nanomaterials and Nanosafety, Institute of High Energy Physics, Chinese Academy of Sciences, Beijing 100049, China, [3]College of Chemistry and Chemical Engineering, Jiangxi Normal University, Nanchang 330022, China.

Computational studies considering both thermodynamic and kinetic aspects revealed that graphyne, a carbon material that has recently been of increasing interest, favours unprecedented homogeneous "in-plane" addition reactions. The addition of dichlorocarbene to the C(*sp*)-C(*sp*) bond, a site with outstanding regioselectivity in graphyne, proceeds via a stepwise mechanism. Due to their homogeneous nature, additions occurring at C(*sp*)-C(*sp*) bonds yield structurally ordered two-dimensional carbon compounds (2DCCs). 2DCCs have electronic band structures near the Fermi level that are similar to those of graphene and are either electrically semi-conductive or metallic depending on whether the reactions break the hexagonal symmetry. Notably, 2DCCs can be further functionalised through substitution reactions with little damage to the extended π-electron conjugation system. These results suggest that 2DCCs derived from graphyne have physical properties comparable to those of graphene and chemical properties superior to those of graphene. Therefore, 2DCCs are expected to be better suited to practical applications.

Carbon is able to make chemical bonds with nearly all elements in the periodic table, including itself. It can adopt three types of hybridisation, *sp*, sp^2 and sp^3. These types of hybridisation result in the formation of carbon geometries with linear, trigonal planar and tetrahedral shapes, respectively. Among hybridised carbons, sp^3 carbons form σ bonds with electrons that are primarily confined to the vicinity of the carbons, whereas *sp* and sp^2 carbons form conjugated π bonds with delocalised electrons. This versatile bonding ability makes carbon the key building atom for organic compounds, which are the basis of not only life but also modern organic electronics.

The first characterised carbon allotrope consisting of sp^2 carbon is graphite. Graphite has a planar, multi-layered structure, with each layer consisting of sp^2 carbons arranged in a hexagonal lattice. It exists abundantly in nature and has a variety of uses, e.g., as pencil lead, lubricants and anodes in battery technologies. Polyacetylene is a stable organic polymer with repeating sp^2 carbon dimers (HC=CH) along the polymer chain that is electrically semi-conductive. After functional doping, the conductivity of polyacetylene can be strikingly increased[1], and therefore this polymer is well known as an "electrically conductive plastic". In addition to graphite and polyacetylene, sp^2 carbon atoms are found in polycyclic aromatic hydrocarbons (PAHs)[2], which are two-dimensional organic π-systems with sizes ranging from several to several tens of nanometers. PAHs have served as important models for molecular orbital theory and spectroscopy and also have potential applications in organic electronics. Experimental observations of fullerenes in 1985[3], carbon nanotubes (CNTs) in 1991[4] and graphene in 2004[5] spurred renewed interest in sp^2 carbon materials. Because of their unprecedented structures, electronic properties and versatility in applications, fullerenes, CNTs and graphene have attracted intense and sustained interest in multidisciplinary fields in recent decades.

These sp^2 carbon materials have a common feature: with the exception of polyacetylene, these materials have molecular surfaces that consist almost entirely of sp^2 carbon atoms forming extended π-electron conjugation systems, which provide the foundation for their intriguing electronic properties. Chemical functionalisation of these materials is usually necessary prior to practical use. For example, the solubility of sp^2 carbon materials must be increased to permit their use in biological systems. Depending on their structural composition, sp^2 carbon materials can be functionalised via chemical addition reactions in which the carbon atoms are converted from sp^2 to sp^3 hybrids to bond with the chemical groups being added. Such addition reactions unavoidably disrupt the

extended π-conjugation system (Figure 1a). The deterioration of π-conjugation can severely damage the electronic performance, which is based on the conjugated system. For example, after solubilisation via oxidation reactions, the electrical conductivity of CNTs and graphene may be reduced by more than a thousandfold. Furthermore, addition reactions on sp^2 materials such as graphene usually proceed in an aggregate manner, making the functionalisation process difficult to control.

In this work, we propose a new type of two-dimensional carbon compound (2DCC, Figure 1b). 2DCCs have large extended π-conjugation systems and electronic properties similar to those of graphene. Unlike graphene, they may have intrinsic components suitable for chemical substitution reactions (*e.g.*, the H and OH groups in **III** and **IV** are substitutable, Figure 1b). Consequently, 2DCCs can be functionalised through chemical substitution rather than addition, therefore eliminating the loss of π-conjugation. Structurally, these 2DCCs can be viewed as derivatives of graphyne, a known 2D carbon sheet consisting of *sp* and sp^2 carbon atoms[6–8]. By considering both thermodynamic and kinetic aspects, we computationally studied addition and multiple addition reactions of graphyne. For the first time, we found that graphyne favours homogeneous "in-plane" addition reactions, which can lead to the formation of 2DCCs. The resulting 2DCCs can be semi-conductive or metallic depending on whether the additions break the hexagonal symmetry. After functionalisation via chemical substitution reactions, these 2DCCs retain electronic band structures near the Fermi level. For example, 2DCC **IV** (Figure 1b) is expected to exhibit considerable electric conductivity and aqueous solubility simultaneously, making it suitable for use in biological systems and under other aqueous conditions. This simultaneous electric conductivity and aqueous solubility is a new feature not shared by conventional sp^2 carbon materials. The results suggest that 2DCCs are a conceptually new family of carbon materials that have physical properties comparable to those of graphene and chemical properties superior to those of graphene. Therefore, 2DCCs are expected to be better suited to chemical tailoring and applications.

Results

Homogeneous "in-plane" reactivity. 2DCCs can be regarded as derivatives of graphyne, a 2D material consisting of *sp* and sp^2 carbon atoms[6]. Although the structural and electronic properties of graphyne have been extensively studied experimentally and theoretically[9–16], only a few studies have been devoted to its chemical properties[17]. Therefore, we first studied the reactivity of graphyne to explore the feasibility of deriving 2DCCs from this material. The *sp* and sp^2 carbons of graphyne can form three types of carbon-carbon bonds: *sp*-*sp*, *sp*-sp^2 and sp^2-sp^2. All of these bond types can be found in β-graphyne (Figure 2a). Therefore, we first focused on β-graphyne in the reactivity study. For simplicity and without loss of generality, the epoxidation reaction of β-graphyne was considered first.

The addition of one oxygen atom into a unit cell of β-graphyne may yield four possible atomic arrangements. Figures 2b and 2c show configurations with oxygen added to the carbon triple bond (*sp*-*sp*), while Figures 2d and 2e show those with oxygen added to the *sp*-sp^2 and sp^2-sp^2 bonds, respectively. The epoxidation of the *sp*-sp^2 and sp^2-sp^2 bonds gives "*on-top*" products, with oxygen protruding upwards from the basal plane of graphyne (Figures 2d and 2e). This "on-top" configuration is characteristic of addition products of sp^2 carbon materials and has previously been reported for fullerenes[18], carbon nanotubes[19] and graphene[20]. In sharp contrast, the epoxidation of *sp*-*sp* bonds yields amazing "*in-plane*" products in which the oxygen lies within the basal plane of graphyne (Figures 2b and 2c). This "in-plane" configuration perfectly maintains the planarity of pristine graphyne. Interestingly, the "in-plane" configuration shown in Figure 2b is thermodynamically more stable than the "on-top" configurations: (b) is lower in energy than (d) and (e) by 15.4 and 21.2 kcal·mol^{-1} per unit cell, respectively. The "in-plane" structure of (c) is thermodynamically less stable than that of (b) by

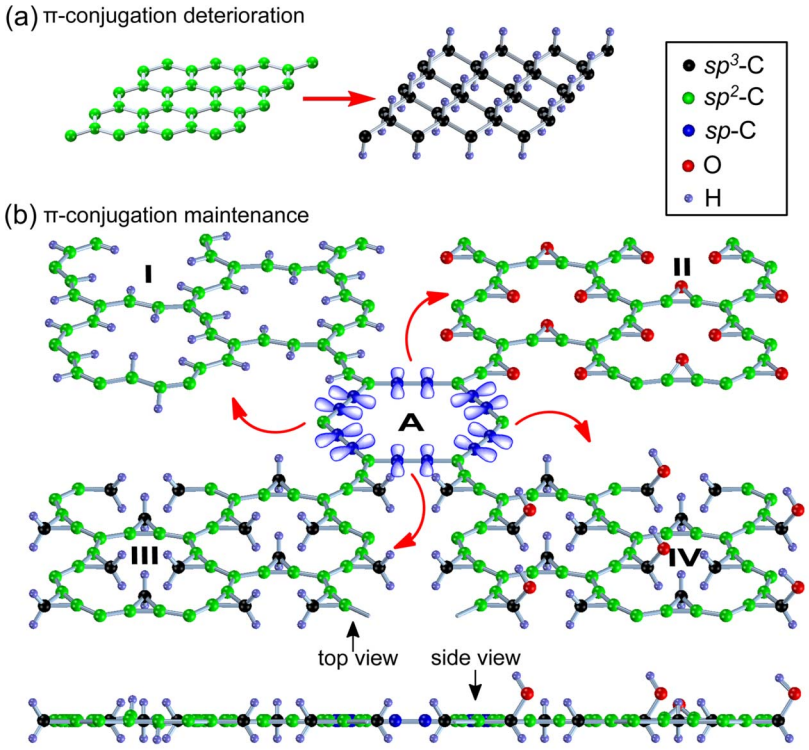

Figure 1 | (a) The deterioration of π-electron conjugation in graphene unavoidably caused by chemical addition reactions. (b) The maintenance of π-electron conjugation in 2DCCs (**I**, **II**, **III**, **IV**) derived from α-graphyne (**A**) via "in-plane" addition reactions. In (a) and (b), the p_y atomic orbitals of *sp*-C are shown, whereas the p_z orbitals of *sp*-C and sp^2-C are not shown for clarity.

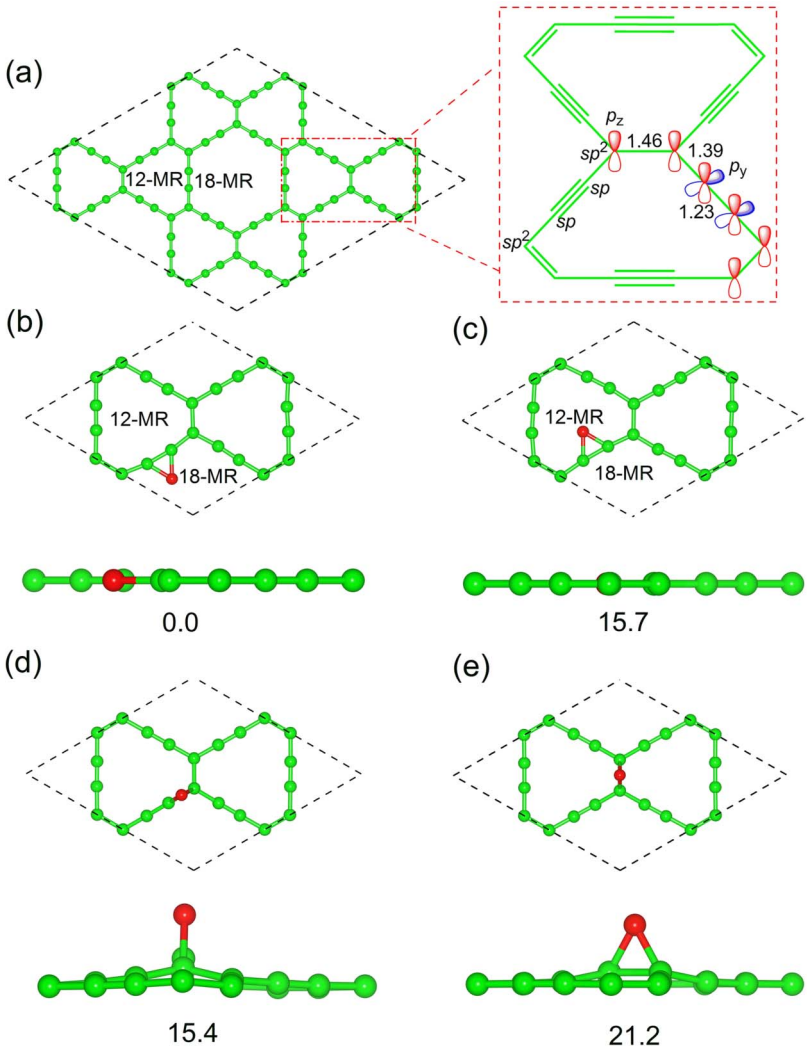

Figure 2 | Thermodynamic selectivity of the oxygenation of β-graphyne. (a) Schematic structure of β-graphyne, with the right panel showing bond lengths (in Å), atom types and atomic orbitals for selected carbons. (b), (c), (d) and (e) Top and side views of the products of β-graphyne oxygenation with the relative energies (kcal·mol^{-1}). MR in (a) and (b) is the abbreviation for "membered ring". C, green; O, red.

15.7 kcal·mol^{-1}. Obviously, the lower stability of (c) relative to (b) can be ascribed to that the additional oxygen in (c) is located in a 12-membered ring (12-MR), whereas the oxygen in (b) is in an 18-membered ring (18-MR). Therefore, (c) is more sterically hindered than (b). The "on-top" configuration (e) is less stable than the "on-top" configuration (d) by 5.8 kcal·mol^{-1}. This result is in agreement with the fact that (d) is produced by addition to the *sp*-sp^2 carbon bond of graphyne, which is more chemically "unsaturated" than the sp^2-sp^2 bond, the addition site for (e).

The thermodynamic selectivity for addition to various bonds is in accordance with the bond lengths. The lengths of the *sp*-*sp*, *sp*-sp^2 and sp^2-sp^2 bonds in β-graphyne are calculated to be 1.23, 1.39 and 1.46 Å, respectively (Figure 2a). For these bonds, a shorter bond length indicates a greater degree of chemical unsaturation, and consequently, greater reactivity. Reactions occurring at the shortest *sp*-*sp* bonds thus release the most energy and result in the most thermodynamically stable adducts. The right panel of Figure 2a shows the unhybridised p_y and p_z orbitals for representative carbons of β-graphyne. All p_y orbitals are orthogonal to p_z orbitals. The p_z orbitals are perpendicular to the basal plane of graphyne, are distributed on all carbons and contribute to the extended π-electron conjugation system; the p_y orbitals lie in the basal plane of graphyne and are distributed only on *sp* carbons. During the "in-plane" additions, the adatoms react only with the p_y orbitals of *sp* carbons, resulting in little change to the orthogonal p_z orbitals and the extended π-electron conjugation. Therefore, "in-plane" reactions provide a unique approach to the covalent functionalisation of graphyne while simultaneously maintaining electronic properties near the Fermi level. This behaviour is in sharp contrast to that of conventional sp^2 carbon materials such as fullerenes, carbon nanotubes and graphene, for which any covalent functionalisation severely changes their electronic properties.

We further studied the kinetic selectivity of the three different carbon-carbon bonds of graphyne by investigating their reactions with dichlorocarbene (CCl_2), a reactive species that has been previously used for the functionalisation of fullerenes and carbon nanotubes[21,22]. Similar to oxygenation (Figures 2b–2d), four sites in β-graphyne are able to form unique products with CCl_2. These sites are labelled **1** through **4** in the cluster model of graphyne (insert of Figure 3). The corresponding products are denoted as **p1** through **p4**. Since the solvent effect and biradical character were found to have slight influences on the reaction barriers and thermodynamics for dichlorocarbene additions (Fig. S1 and Table S1 of Supplementary Information), we will focus on the reaction pathways in the gas phase in the following discussion. As shown in Figure 3, **p1**, in which the CCl_2 group is added to site **1** (*i.e.*, the *sp*-*sp* bond) and located in the 18-MR side, has the greatest exothermicity, with a reaction energy (E_r) of −56.2 kcal·mol^{-1}. The E_r values of **p2**, **p3** and **p4**

are approximately 18.0, −35.8 and −39.8 kcal·mol^{-1}, respectively. The thermodynamic preference of CCl_2 for reacting with the *sp-sp* bond from the 18-MR side was confirmed by extended-model calculations with periodic boundary conditions (Supplementary Fig. S3), in good agreement with the above results for graphyne oxygenation. The E_r of 18.0 kcal·mol^{-1} for **p2** suggests that the formation of **p2** is not thermodynamically favoured. This thermodynamic unfavourability can be ascribed to the high steric repulsion encountered when inserting a CCl_2 group into a small 12-MR.

According to Figure 3, the most convenient pathway to **p1** corresponds to a stepwise mechanism. In the first step, CCl_2 approaches the *sp-sp* bond to form intermediate **int1** via transition state **ts1**. The activation energy ($E^{\neq}$) of this step is 6.5 kcal·mol^{-1}. In **int1**, the CCl_2 moiety is nearly perpendicular to the graphyne plane. In the second step, the CCl_2 of **int1** rotates to lie in the 18-MR to form **p1** with an activation energy of 3.2 kcal·mol^{-1}. The small $E^{\neq}$ of both steps suggests that the formation of **p1** via the reaction of CCl_2 and graphyne is very facile. Figure 3 also shows the reaction paths for **p3** and **p4**: **p4** is linked to **p3** via **ts3**, with $E^{\neq}$ = 26.8 kcal·mol^{-1}; **p3** is linked to **int1** via **ts4**, with $E^{\neq}$ = 11.2 kcal·mol^{-1}. Thus, **p3** and **p4**, if formed, will readily transform into **p1** upon thermal annealing. Hence, the formation of **p1** is uniquely favoured with respect to both thermodynamic and kinetic aspects, suggesting that the *sp-sp* bond of β-graphyne is highly regioselective in chemical reactions. A similarly high regioselectivity is also observed for the *sp-sp* bond of α-graphyne (Supplementary Fig. S4).

Another important issue regarding graphyne reactivity is its regioselectivity in multiple addition reactions. Reportedly, sp^2 carbon materials (fullerenes, carbon nanotubes and graphene) thermodynamically favour an inhomogeneous mode of multiple additions in which chemical groups tend to be added aggregately so as to destroy fewer π-bonds and maintain a larger π-conjugated area[23,24]. Such inhomogeneous additions yield products consisting of separated areas of sp^2 and sp^3 carbons. Because the "in-plane" addition reactions of graphyne cause no damage to the π-electron conjugation system, the inhomogeneous mode should not predominate for graphyne.

Indeed, we observed that graphyne tends to undergo multiple addition reactions homogeneously. Depending on their orientations, the *sp-sp* bonds of α-graphyne can be classified into three groups: **sites I**, **II** and **III**, which are perpendicular to the three arrows in Figure 4a. To study multiple additions, we added four H_2 molecules to four *sp-sp* bonds of a 2 × 2 supercell of α-graphyne using different combinations of the three types of *sp-sp* bonds. The addition of H_2 to two adjacent *sp-sp* bonds of α-graphyne can occur in two different ways, yielding the armchair (Figure 4b) and zigzag (Figure 4c) configurations for the hydrogenated carbon chains. The armchair configuration (Figure 4b) was found to be lower in energy than the zigzag one (Figure 4c) by 0.9 kcal·mol^{-1}. Consequently, we focused on the armchair configurations when adding four H_2. We exhausted the armchair products and then calculated their energies after full geometry optimisations (Supplementary Fig. S5). Figure 4d presents the results. Along the abscissa app:addword:abscissaof Figure 4d, $\mathbf{4S_I}$

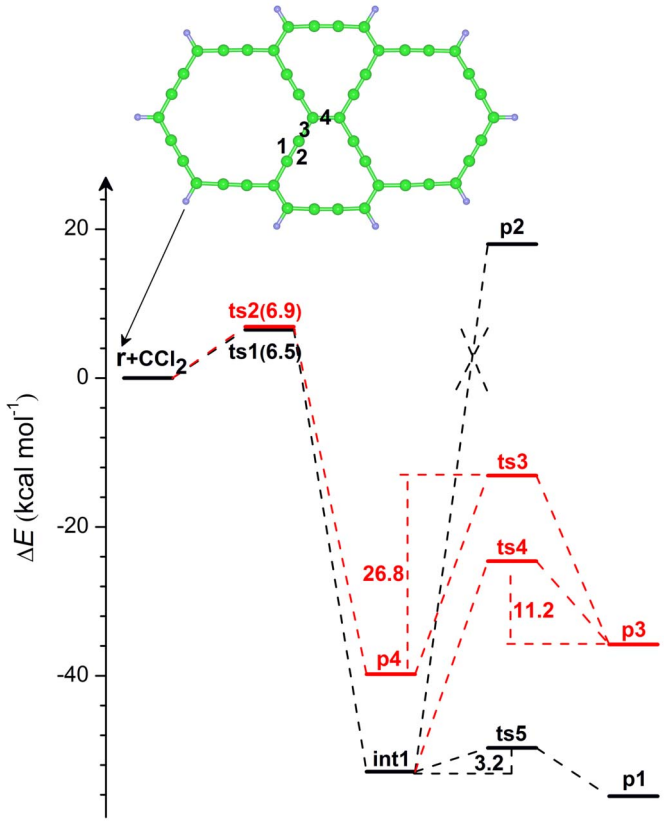

Figure 3 | Energy profiles for CCl_2 additions to α-graphyne calculated with the B3LYP/6-31G(d) method. The insert panel shows the cluster model of graphyne used in the calculations. Numbers **1** through **4** denote the addition sites; **p1** through **p4** represent the products in which CCl_2 was added to sites **1** through **4**, respectively. The unit of energy is kcal·mol^{-1}. C, green; Cl, brown; H, light blue.

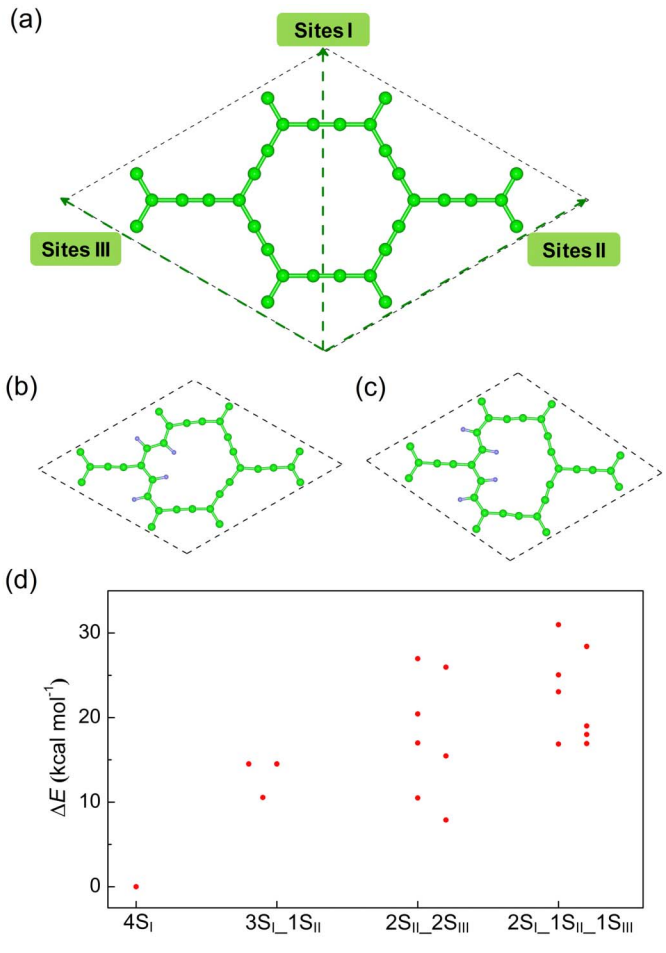

Figure 4 | Thermodynamic selectivity of multiple hydrogenations of α-graphyne. (a) Sites I, II and III represent three groups of *sp-sp* bonds perpendicular to the dashed arrow lines. (b) and (c) are two different atomic arrangements for H_2 additions occurring at neighbouring *sp-sp* bonds. (d) Relative energies of the products with four H_2 molecules added to the different positions of a 2 × 2 supercell of α-graphyne. C, green; H, light blue.

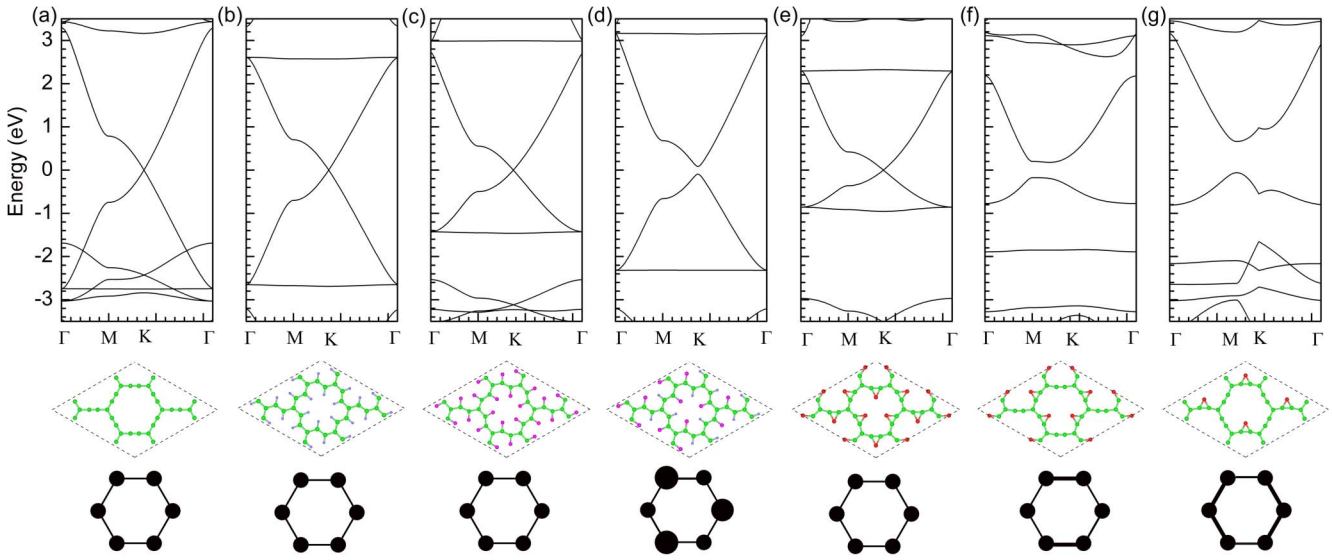

Figure 5 | Electronic band structures of α-graphyne and 2DCCs. (a) α-graphyne, (b) H-2DCC, (c) F-2DCC, (d) HF-2DCC, (e) O-2DCC, (f) $O_{2/3}$-2DCC and (g) $O_{1/3}$-2DCC. In each figure, the top panel shows the electronic band structures calculated by DFT methods, the middle panel shows the 2 × 2 supercell of the structure, and the bottom panel shows the symmetry of the hexagonal lattice. C, green; H, light blue; F, magenta; O, red.

corresponds to the products in which the four H_2 were all added to **site I** *sp-sp* bonds; $\mathbf{3S_I–1S_{II}}$ represents the products with three and one H_2 added to **site I** and **site II**; $\mathbf{2S_{II}–2S_{III}}$ denotes the products with the four H_2 added equally to **site II** and **site III**; and $\mathbf{2S_I–1S_{II}–1S_{III}}$ are the products with two H_2 added to **site I** and one each added to **site II** and **site III**, respectively. The numbers of symmetrically unique products belonging to the series of $\mathbf{4S_I}$, $\mathbf{3S_I–1S_{II}}$, $\mathbf{2S_{II}–2S_{III}}$ and $\mathbf{2S_I–1S_{II}–1S_{III}}$ were found to be 1, 3, 7 and 8. This increase in the number of products is consistent with the fact that more types of *sp-sp* bonds are reacted in the products along the series. Figure 4d shows that the relative energies of the products also tend to increase along this series. For graphyne, additions involving fewer types of *sp-sp* bonds result in greater structural homogeneity. Therefore, these data suggest an interesting result that graphyne prefers a homogeneous mode of multiple addition reactions. This preference is in sharp contrast to that of conventional carbon materials. For example, the lowest-energy product $\mathbf{4S_I}$ (corresponding to four H_2 added to the four horizontal *sp-sp* bonds of Figure 4a) has the most homogeneous distribution of hydrogens among all the products. The energy barrier for the addition of H_2 to the *sp-sp* bond of graphdiyne has been estimated to be 48.4 kcal·mol^{-1}. Therefore, it is predicted that the hydrogenation of graphdiyne by H_2 requires a catalytic pathway[25]. Considering the similarity of the *sp-sp* bonds of graphyne to those of graphdiyne, a similar catalytic pathway is likely necessary for the hydrogenation of graphyne.

We further investigated the mobility of oxygen atoms in oxygenated α-graphyne. The $E^{\neq}$ for O to migrate from one *sp-sp* bond to a neighbouring bond was calculated to be 24.2 kcal·mol^{-1}, whereas the $E^{\neq}$ for O to rotate 180° about the *sp-sp* bond was 15.6 kcal·mol^{-1} (Supplementary Information). These results suggest that thermodynamically unfavourable products such as $\mathbf{3S_I–1S_{II}}$, $\mathbf{2S_{II}–2S_{III}}$ and $\mathbf{2S_I–1S_{II}–1S_{III}}$ can be readily converted into $\mathbf{4S_I}$ via thermal annealing.

Electronic band gap tuning. Owing to the zero band gap of graphene, graphene transistors have small on/off ratios, typically less than ten[26]. As a result, graphene transistors are hard to turn off, preventing their application in electronic devices. Chemical addition reactions such as hydrogenation[27] and oxidation[28] have been proposed to open the band gap of graphene. To open large band gaps by these reactions, dispersive additions following certain patterns are required[29–31]. However, because graphene thermodynamically prefers aggregate additions[24,32], the gap-opening process is difficult to control. Moreover, since this gap opening occurs at the expense of the conversion of the carbons of graphene from sp^2 to sp^3 hybrids, the electron mobility of graphene deteriorates severely after gap opening.

Graphyne also has the gapless problem[10,11]. Here, we predicted that the band gap opening of graphyne can be achieved via hexagonally asymmetric addition reactions. Due to the homogeneous "in-plane" reactivity of graphyne, such gap opening should be easy to control and free from substantial electron-mobility reduction. Figures 5a–5e show the 2 × 2 hexagonal supercells and electronic band structures of α-graphyne, H-2DCC, F-2DCC, HF-2DCC and O-2DCC (see, respectively, the middle and top panels for each species). The latter four species are derivatives of α-graphyne obtained by full hydrogenation, full fluorination, combined hydrogenation and fluorination and oxygenation of the *sp-sp* bonds, respectively. Figures 5f and 5g correspond to $O_{2/3}$-2DCC and $O_{1/3}$-2DCC, which are derivatives of α-graphyne with 2/3 and 1/3 of the *sp-sp* bonds oxygenated. All structures were fully relaxed before the band gap calculations were performed.

As shown in Figure 5, H-2DCC, F-2DCC and O-2DCC have electronic band structures similar to those of α-graphyne near the Fermi level: CBM and VBM meet at the K points of the Brillouin zone that are donated as Dirac points, yielding zero band gaps. The Fermi velocities (v_F) and effective masses of holes (m_h*) and electrons (m_e*) near the Dirac points along the K-Γ direction were estimated for α-graphyne, H-2DCC, F-2DCC and O-2DCC. As listed in Table 1, the Fermi velocities for these species are approximately 6.34×10^5, 5.67×10^5, 4.72×10^5 and 3.27×10^5 m/s, respectively, which are smaller than that of graphene, ~10^6 m/s[33]. The m_h* and m_e* of graphyne and graphyne derivatives are larger than those obtained experimentally for graphene[5]. Interestingly, the band gaps of HF-2DCC, $O_{2/3}$-2DCC and $O_{1/3}$-2DCC are open, with gap sizes of 0.2, 0.4 and 0.7 eV, respectively. Although the gap is open, the band structure of HF-2DCC resembles that of α-graphyne. Even the band structures of $O_{2/3}$-2DCC and $O_{1/3}$-2DCC have some features in common with that of α-graphyne (Figure 5). These results demonstrate the fascinating characteristics of "in-plane" addition reactions, which tune the band gaps of graphyne while maintaining its main electronic properties. This ability is in agreement with the above

Table 1 | Calculated Fermi velocities (v_F) and effective masses of holes and electrons (m_h* and m_e*) near the Dirac points along the K-Γ direction for α-graphyne, H-2DCC, F-2DCC and O-2DCC. The Fermi velocity and effective masses of carriers for graphene are taken from ref. 33 and 5

	graphene	α-graphyne	H-2DCC	F-2DCC	O-2DCC
v_F(m/s)	~10^6	6.34×10^5	5.67×10^5	4.72×10^5	3.27×10^5
m_h*(m_0)	~0.06	0.34	0.77	0.93	1.74
m_e*(m_0)	~0.03/~0.1	0.32	0.77	0.69	1.04

finding that "in-plane" addition reactions have little effect on the p_z orbitals and the extended π-electron conjugation system of graphyne.

The band gap openings of HF-2DCC, $O_{2/3}$-2DCC and $O_{1/3}$-2DCC can be understood based on their non-hexagonally symmetric addition patterns. For HF-2DCC, the additions of H and F divide the six corner carbons of α-graphyne's 18-MR into two types with different chemical environments: one is $C(CH)_3$, *i.e.*, an sp^2 carbon bonded to three CH units, and the other is $C(CF)_3$, *i.e.*, an sp^2 carbon bonded to three CF units. By contrast, the chemical environments of the six edges of the 18-MR are identical, with each edge consisting of a C-C(H)-C(F)-C unit linked to two other such units through a shared carbon. Therefore, the symmetry-breaking pattern of HF-2DCC can be represented by the bottom panel of Figure 5d, in which the corners belong to two different types while the six edges are identical. In terms of $O_{2/3}$-2DCC, the six corner carbons of the 18-MR are symmetrically identical, whereas the edges can be classified into two types, with and without oxygen. Therefore, $O_{2/3}$-2DCC has a different symmetry-breaking pattern, as shown in the bottom of Figure 5f. Similarly, one can understand the symmetry-breaking pattern for $O_{1/3}$-2DCC and that the additions in H-2DCC, F-2DCC and O-2DCC do not break the hexagonal symmetry. Therefore, according to Figure 5, the band gap openings of HF-2DCC, $O_{2/3}$-2DCC and $O_{1/3}$-2DCC can be ascribed to their hexagonally asymmetric addition patterns, whereas the band gap closings of H-2DCC, F-2DCC and O-2DCC can be ascribed to the hexagonal symmetry of their addition patterns. A similar symmetry-breaking mechanism for band gap opening also holds for graphene[34,35] and has been previously used to open graphene's band gap.

The band gap evolution of graphyne with respect to the extent of addition reactions is strikingly different from that of graphene. When graphene is fully reacted with chemical addition groups, the resulting products have a wide band gap. For example, the band gap of fully hydrogenated graphene (*i.e.*, graphane) is over 4.0 eV, being electrically insulating[36,37]. By contrast, a metallic to semiconductive to metallic evolution with respect to the extent of "in-plane" additions was predicted for α-graphyne. Figures 5a, 5g, 5f and 5d show this evolution for graphyne upon oxygenation. Based on the homogeneous, "in-plane" reactivity of graphyne and the hexagonally asymmetric addition patterns required for band gap opening, one can expect that $O_{1/3}$-2DCC (Figure 5g) will have the largest band gap (0.7 eV) among the species derived from α-graphyne by "in-plane" addition of oxygen. It is worth noting that $O_{1/3}$-2DCC is simultaneously the most thermodynamically stable structure among those with 1/3 of the *sp-sp* bonds are oxygenated (Figure 4 and corresponding discussion). Therefore, one can further expect that such consistency between the size of the band gap and the extent of the thermodynamic stability, which never exists in graphene, will increase the relative feasibility of band gap tuning of graphyne.

Discussion

The above thermodynamic and kinetic data consistently suggest the high regioselectivity of the *sp-sp* bonds in graphyne. These bonds undergo homogeneous "in-plane" addition reactions, perfectly maintaining the planarity of graphyne without damaging the extended π-electron conjugation system. Therefore, graphyne can serve as an ideal precursor to produce structurally ordered 2DCCs, whose electronic structures are predicted to be semi-conductive or metallic depending on whether the additions break the hexagonal symmetry. Interestingly, the "in-plane" addition of chemical species with substitutable groups to graphyne, such as CCl_2 and CH_2, yields 2DCCs capable of undergoing substitution reactions. Substitution reactions can also be used to adjust the band gap of graphyne according to the same hexagonal-symmetry breaking mechanism while causing little deterioration to the extended π-electron conjugation system. These chemical properties are not shared by conventional sp^2 carbon materials such as graphene. The results suggest that 2DCCs are a conceptually new family of carbon materials with physical properties comparable to those of graphene and chemical properties superior to those of graphene. Therefore, 2DCCs are expected to be better suited for chemical tailoring and practical applications.

Methods

Geometry optimisation and electronic structure calculations were performed with the Vienna Ab-initio Simulation Package (VASP)[38]. The generalized gradient approximation (GGA) with the exchange-correlation functional of the Perdew-Burke-Ernzerhof functional (PBE)[39] was employed. The ion-electron interaction was described using the projector-augmented wave method[40] with a kinetic energy cut-off of 500 eV, and the convergence criterion in the self-consistency process was set to 10^{-5} eV. The vacuum space along the Z direction was 15 Å, which is sufficiently large to prevent interaction between the nearest images. For the geometry optimisations of a unit cell and a 2×2 supercell, $7 \times 7 \times 1$ and $3 \times 3 \times 1$ Monkhorst-Pack meshes[41] of k points were used, respectively, to sample the first Brillouin zone. All lattice constants and coordinates were fully relaxed until all atomic forces became smaller than 0.01 eV/Å.

The reaction paths for dichlorocarbene additions and isomerisations of O-2DCC were calculated on the basis of a cluster model using the B3LYP hybrid functional with the 6-31G(d) basis set for all atoms, as implemented in the Gaussian 09 package[42]. Analytical frequencies were conducted at the same level of theory for all structures in the reaction paths, which confirmed the structures to be minimal or transition states. Because dichlorocarbene addition and O-2DCC isomerisation usually occur in solvents such as dichlorobenzene and toluene, the respective solvent effects were further evaluated via single-point (SP) energy calculations with the polarisable continuum model (PCM)[43] using B3LYP/6-31G(d)-optimised geometries. For dichlorocarbene additions, energy profiles considering a biradical character and the effect of a larger basis set were also computed via SP calculations. The results of these SP calculations are presented in Fig. S1, Table S1 and Table S2 of the Supplementary Information.

1. Chiang, C. K. *et al.* Electrical conductivity in doped polyacetylene. *Phys. Rev. Lett.* **39**, 1098–1101 (1977).
2. Randić, M. Aromaticity of polycyclic conjugated hydrocarbons. *Chem. Rev.* **103**, 3449–3605 (2003).
3. Kroto, H. W., Heath, J. R., O'Brien, S. C., Curl, R. F. & Smalley, R. E. C60: Buckminsterfullerene. *Nature* **318**, 162–163 (1985).
4. Iijima, S. Helical microtubules of graphitic carbon. *Nature* **354**, 56–58 (1991).
5. Novoselov, K. S. *et al.* Electric field effect in atomically thin carbon films. *Science* **306**, 666–669 (2004).
6. Baughman, R. H., Eckhardt, H. & Kertesz, M. Structure property predictions for new planar forms of carbon: Layered phases containing sp2 and sp atoms. *J. Chem. Phys.* **87**, 6687–6699 (1987).
7. Bunz, U. H. F., Rubin, Y. & Tobe, Y. Polyethynylated cyclic π-systems: scaffoldings for novel two and three-dimensional carbon networks. *Chem. Soc. Rev.* **28**, 107–119 (1999).
8. Diederich, F. Carbon scaffolding: buildind acetylenic all-carbon and carbon-rich compounds. *Nature* **369**, 199–207 (1994).
9. Narita, N., Nagai, S., Suzuki, S. & Nakao, K. Optimized geometries and electronic structures of graphyne and its family. *Phys. Rev. B* **58**, 11009–11014 (1998).

10. Malko, D., Neiss, C., Vines, F. & Gorling, A. Competition for graphene: Graphynes with direction-dependent dirac cones. *Phys. Rev. Lett.* **108**, 086804 (2012).
11. Kim, B. G. & Choi, H. J. Graphyne: Hexagonal network of carbon with versatile Dirac cones. *Phys. Rev. B* **86**, 115435 (2012).
12. Kehoe, J. M. *et al.* Carbon networks based on dehydrobenzoannulenes. 3. Synthesis of graphyne substructures. *Org. Lett.* **2**, 969–972 (2000).
13. Haley, M. M. Synthesis and properties of annulenic subunits of graphyne and graphdiyne nanoarchitectures. *Pure Appl. Chem.* **80**, 519–532 (2008).
14. Li, G. *et al.* Architecture of graphdiyne nanoscale films. *Chem. Commun.* **46**, 3256–3258 (2010).
15. Diederich, F. & Kivala, M. All-carbon scaffolds by rational design. *Adv. Mater.* **22**, 803–812 (2010).
16. Kang, J., Li, J., Wu, F., Li, S.-S. & Xia, J.-B. Elastic, electronic, and optical properties of two-dimensional graphyne sheet. *J. Phys. Chem. C* **115**, 20466–20470 (2011).
17. Wu, P., Du, P., Zhang, H. & Cai, C. Graphyne as a promising metal-free electrocatalyst for oxygen reduction reactions in acidic fuel cells: A DFT Study. *J. Phys. Chem. C* **116**, 20472–20479 (2012).
18. Heymann, D. *et al.* $C_{60}O_3$, a fullerene ozonide: Synthesis and dissociation to $C_{60}O$ and O_2. *J. Am. Chem. Soc.* **122**, 11473–11479 (2000).
19. Lu, X., Yuan, Q. & Zhang, Q. Sidewall epoxidation of single-walled carbon nanotubes: A theoretical prediction. *Org. Lett.* **5**, 3527–3530 (2003).
20. Kim, S. *et al.* Room-temperature metastability of multilayer graphene oxide films. *Nat. Mater.* **11**, 544–549 (2012).
21. Liu, C. *et al.* Carbene-functionalized single-walled carbon nanotubes and their electrical properties. *Small* **7**, 1257–1263 (2011).
22. Hu, H. *et al.* Sidewall functionalization of single-walled carbon nanotubes by addition of dichlorocarbene. *J. Am. Chem. Soc.* **125**, 14893–14900 (2003).
23. Wang, L. *et al.* Stability of graphene oxide phases from first-principles calculations. *Phys. Rev. B* **82**, 161406 (2010).
24. Gao, X., Zhao, Y., Liu, B., Xiang, H. & Zhang, S. B. π-Bond maximization of graphene in hydrogen addition reactions. *Nanoscale* **4**, 1171–1176 (2012).
25. Psofogiannakis, G. M. & Froudakis, G. E. Computational prediction of new hydrocarbon materials: The hydrogenated forms of graphdiyne. *J. Phys. Chem. C* **116**, 19211–19214 (2012).
26. Reid, T. Graphene: Switch if off. *Nat. Nanotechnol.* (2008).
27. Balog, R. *et al.* Bandgap opening in graphene induced by patterned hydrogen adsorption. *Nat. Mater.* **9**, 315–319 (2010).
28. Nourbakhsh, A. *et al.* Bandgap opening in oxygen plasma-treated graphene. *Nanotechnology* **21**, 435203 (2010).
29. Pedersen, T. G. *et al.* Graphene antidot lattices: Designed defects and spin qubits. *Phys. Rev. Lett.* **100**, 136804 (2008).
30. Martinazzo, R., Casolo, S. & Tantardini, G. F. Symmetry-induced band-gap opening in graphene superlattices. *Phys. Rev. B* **81**, 245420 (2010).
31. Gao, X., Wei, Z., Meunier, V., Sun, Y. & Zhang, S. B. Opening a large band gap for graphene by covalent addition. *Chem. Phys. Lett.* **555**, 1–6 (2013).
32. Sun, T. & Fabris, S. Mechanisms for oxidative unzipping and cutting of graphene. *Nano. Lett.* **12**, 17–21 (2012).
33. Avouris, P., Chen, Z. & Perebeinos, V. Carbon-based electronics. *Nat. Nanotechnol.* **2**, 605–615 (2007).
34. Peng, X. & Ahuja, R. Symmetry breaking induced bandgap in epitaxial graphene layers on SiC. *Nano. Lett.* **8**, 4464–4468 (2008).
35. Dong, X. *et al.* Symmetry breaking of graphene monolayers by molecular decoration. *Phys. Rev. Lett.* **102**, 135501 (2009).
36. Sofo, J. O., Chaudhari, A. S. & Barber, G. D. Graphane: A two-dimensional hydrocarbon. *Phys. Rev. B* **75**, 153401 (2007).
37. Lebègue, S., Klintenberg, M., Eriksson, O. & Katsnelson, M. I. Accurate electronic band gap of pure and functionalized graphane from GW calculations. *Phys. Rev. B* **79**, 245117 (2009).
38. Kresse, G. & Furthmuller, J. Efficient iterative schemes for ab initio total-energy calculations using a plane-wave basis set. *Phys. Rev. B* **54**, 11169–11186 (1996).
39. Perdew, J. P., Burke, K. & Ernzerhof, M. Generalized gradient approximation made simple. *Phys. Rev. Lett.* **77**, 3865–3868 (1996).
40. Kresse, G. & Joubert, D. From ultrasoft pseudopotentials to the projector augmented-wave method. *Phys. Rev. B* **59**, 1758–1775 (1999).
41. Monkhorst, H. J. & Pack, J. D. Special points for Brillouin-zone integrations. *Phys. Rev. B* **13**, 5188–5192 (1976).
42. Frisch, M. J. *et al.* Gaussian 09, Revision C.01, Gaussian, Inc.: Wallingford CT, 2010 (see Supplementary Information for full citation).
43. Miertuš, S., Scrocco, E. & Tomasi, J. Electrostatic interaction of a solute with a continuum. A direct utilizaion of ab initio molecular potentials for the prevision of solvent effects. *Chem. Phys.* **55**, 117–129 (1981).

Acknowledgments

This work was supported by the National Key Basic Research Project of China (973 programs: 2012CB934001, 2011CB933403, 2012CB932504, 2012CB720904), the National Natural Science Foundation of China (21171138, 21274164, 21144001), and CAS Hundreds Elite Program (Y2291820S3).

Author contributions

X.G. conceived the initial idea of this research. J.Z. demonstrated the initial idea and collected all data. X.Z. and Y.Z. participated in the discussions. J.Z. and X.G. wrote the paper. X.G. and X.Z. guided the work.

Additional information

Supplementary information accompanies this paper at http://www.nature.com/scientificreports

Competing financial interests: The authors declare no competing financial interests.

License: This work is licensed under a Creative Commons Attribution-NonCommercial-NoDerivs 3.0 Unported License. To view a copy of this license, visit http://creativecommons.org/licenses/by-nc-nd/3.0/

How to cite this article: Zheng, J., Zhao, X., Zhao, Y. & Gao, X. Two-Dimensional Carbon Compounds Derived from Graphyne with Chemical Properties Superior to Those of Graphene. *Sci. Rep.* **3**, 1271; DOI:10.1038/srep01271 (2013).